JOURNAL OF MATERIALS SCIENCE 26 (1991) 4439–4444

Piezoelectric properties of (Pb, Sr) (Zr, Ti, Mn, Zn, Nb)O_3 piezoelectric ceramic

LONG WU, CHICK-KWO LIANG, CHIN-FANG SHIEU
Department of Electrical Engineering, National Cheng Kung University, Tainan, Taiwan

In this paper, the aim is to study the piezoelectric properties of (Pb, Sr)[(Zr, Ti)($Zn_{1/3}Nb_{2/3}$)($Mn_{1/3}Nb_{2/3}$)]O_3 ceramic with compositions close to the morphotropic phase boundary. The dielectric and piezoelectric properties of this system were investigated by way of changed contents of two main compounds, TiO_2 and $Mn_{1/3}Nb_{2/3}$. There are two phases existing in this system, one tetragonal and the other pseudocubic. With a constant amount of 4 mol% $Pb(Mn_{1/3}Nb_{2/3})O_3$ and 8 mol% $Pb(Zn_{1/3}Nb_{2/3})O_3$, the morphotropic phase boundary exists when the amount of $PbTiO_3$ is nearly equal to 44 mol%. The structure is perovskite with pseudocubic symmetry for $PbTiO_3$ less than 44 mol%, but it is tetragonal symmetry for higher $PbTiO_3$ concentrations. The planar coupling factor and piezoelectric constant are higher for compositions near the morphotropic phase boundary, but the mechanical quality factor and longitudinal velocity are lowest. As far as the dielectric constant of poled material is concerned, its maximum in the multicomponent system is displaced into the tetragonal phase and does not coincide with the maximum of electromechanical quality factor. The variation of remanent polarization with composition is the same as that of the coupling factor. Thus, compositions with the tetragonal phase are "ferroelectrically harder" and those with the pseudocubic phase are "ferroelectrically softer" than compositions close to the morphotropic phase boundary. Besides the influence of Ti, the effect of $Mn_{1/3}Nb_{2/3}$ is also studied in this paper. The planar coupling factor increases with increasing $Mn_{1/3}Nb_{2/3}$ and reaches a maximum at 5 mol% $Mn_{1/3}Nb_{2/3}$, and then decreases for higher $Mn_{1/3}Nb_{2/3}$ values. The mechanical quality factor increases, but the dielectric constant decreases, with increasing $Mn_{1/3}Nb_{2/3}$.

1. Introduction

After the fundamental studies on PZT by Jaffe and co-workers, many tentative studies were carried out in order to improve the performance of these ceramics; for instance, the ions of Pb and (Zr, Ti) were partly substituted by other divalent and tetravalent ions, respectively [1–3], or some pentoxides or sesquioxides were added [4–6]. Such additions improve the insulation properties of PZT and in some cases decrease their ageing effect.

In order to reach the requirements of practical applications, a number of minor additives have been added to the ceramics. However, when two kinds of minor additives were added simultaneously, much improved piezoelectric properties could not be obtained. Therefore, ternary solid-solution ceramics are being synthesized in place of the binary ceramics, consisting of a complex perovskite compound; (Zr, Ti) is substituted by $Mg_{1/3}Nb_{2/3}$ [7], $Co_{1/3}Nb_{2/3}$ [8], $Mn_{1/3}Ta_{2/3}$ [9] and $Mn_{1/3}Nb_{2/3}$ [10] to form a ternary ceramic system and eventually a multicomponent system of complex oxides.

In this paper, the aim is to study the piezoelectric properties of (Pb, Sr)[(Zr, Ti)($Zn_{1/3}Nb_{2/3}$)($Mn_{1/3}Nb_{2/3}$)]O_3 with compositions close to the morphotropic phase boundary (MPB). The dielectric and piezoelectric properties of this system were investigated by way of changed contents of two main compounds, TiO_2 and $Mn_{1/3}Nb_{2/3}$. The influence of the structural transition near the MPB region is of special concern.

2. Experimental procedure

The compositions used in this study were

$$Pb_{0.96}Sr_{0.04}[(Ti_xZr_{1-x})_y\,(Mn_{1/3}Nb_{2/3})_z\,(Zn_{1/3}Nb_{2/3})_{0.08}]O_3$$

with $x = 0.38$–0.55, $y = 0.82$–0.88 and $z = 0.04 \sim 0.1$. All the specimens were prepared by conventional ceramic technology. Raw materials were mixed from pure reagent-grade (> 99%) PbO, $SrCO_3$, TiO_2, ZrO_2, Nb_2O_5, $MnCO_3$ and ZnO. Excess 0.5% PbO was added to the solid solution to enhance the formation of a liquid phase, which served as a densification promoter [11]. A mixture of the starting powders homogenized wih acetone was mixed and milled in the ball mill for 4 h. After that, the mixture was dried and calcined at 920 °C for 2 h in an alumina crucible. The reacted material was ground and then pressed into a disc shape under 700 kg cm^{-2}. The size of the green compact was 15 mm in diameter and 1.0–1.2 mm in thickness. The specimens were covered with an

0022-2461/91 $03.00 + .12

alumina crucible and sintered at 1220 and 1230 °C for 3 h. To provide a positive vapour pressure, $PbZrO_3$ with 3 wt % excess PbO was used as the packing powder [12, 13]. After sintering, the lapped and polished samples were printed with silver paste on each surface and fired at 700 °C ready for the poling process. The poling technique was generally to immerse the sample into silicone oil suffering from dielectric breakdown, and poled by $3\,kV\,mm^{-1}$ at 100 °C for 1 h.

In order to determine the crystal structure, crystal system and lattice, the sintered ceramic bodies were polished, and measurements carried out at room temperature by the X-ray diffraction (XRD) method using CuK_α radiation.

By means of a scanning electron microscope (SEM), the free surface of the sintered ceramic body was observed. The mean grain size was calculated by the line intercept method.

The P–E hysteresis loop was observed with a modified Sawyer–Tower circuit [14]. Finally, dielectric and piezoelectric properties were measured with an HP-4192A LF Impedance Analyser with reference to the IRE Standard [15]. By using the Panametrics 5218 ultrasonic thickness gauge, the longitudinal wave velocity was measured in both poled and unpoled piezoelectric ceramic discs. The piezoelectric strain constant d_{33} was measured by a d_{33} meter.

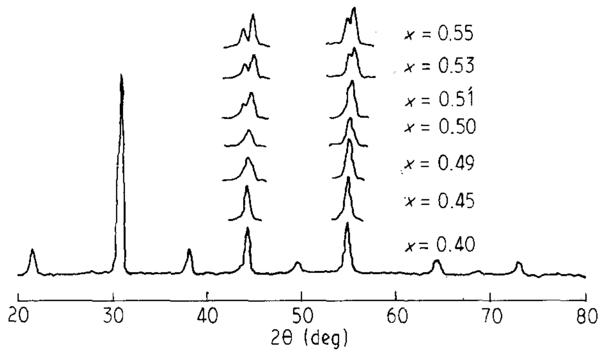

Figure 1 XRD patterns of the $Pb_{0.96}Sr_{0.04}[(Ti_xZr_{1-x})_{0.88}(Mn_{1/3}Nb_{2/3})_{0.04}(Zn_{1/3}Nb_{2/3})_{0.08}]O_3$ system with different x values.

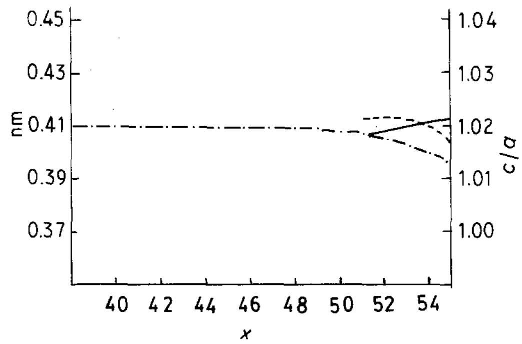

Figure 2 Variation of lattice constants (—·—) a, (---) c and (——) c/a ratio of the $Pb_{0.96}Sr_{0.04}[(Ti_xZr_{1-x})_{0.88}(Mn_{1/3}Nb_{2/3})_{0.04}(Zn_{1/3}Nb_{2/3})_{0.08}]O_3$ system with different x values.

3. Results and discussion

XRD patterns of the $Pb_{0.96}Sr_{0.04}[(Ti_xZr_{1-x})_{0.88}(Mn_{1/3}Nb_{2/3})_{0.04}(Zn_{1/3}Nb_{2/3})_{0.08}]O_3$ system with different x values at room temperature are shown in Fig. 1. In these patterns, no pyrochlore phase can be found. The perovskite phase appears to have pseudocubic symmetry for x less than 0.50, and tetragonal symmetry for x greater than 0.50. A morphotropic transformation between tetragonal and pseudocubic phases was found at x close to 0.50.

In the pseudocubic phase, the lattice constant decreases gradually with an increase of $PbTiO_3$ content, and in the tetragonal phase the lattice constants c and a both decrease with increasing $PbTiO_3$, but the c/a ratio increases with increasing $PbTiO_3$ content (Fig. 2).

All of the compositions were sintered in an air environment with positive Pb atmosphere control at 1220 °C for 3 h. With these sintering conditions, all the samples have a high density near to 94–99% of the theoretical value. Fig. 3 shows the microstructure of sintered samples with different compositions at 1220 °C; the grain size is about 2.5–4.5 μm.

In piezoelectric ceramics, depending on the crystalline phase, the dielectric constant may increase or decrease through poling treatment. In this system the dielectric constant is increased for the tetragonal compositions but decreased for the pseudocubic compositions after poling, as shown in Fig. 4; the results are in agreement with those observed by Isupov and Stolypin [16, 17] and Cross *et al.* [18]. The dielectric constant of this system increases with increase of $PbTiO_3$ until it reaches a peak value at $x = 0.51$, and then decreases for higher $PbTiO_3$ content.

As far as the dielectric constant of poled ceramic is concerned, the maximum point of dielectric constant in the multicomponent system is displaced into the tetragoanl phase and does not coincide with the maximum point of the electromechanical coupling factor. The reasons for this displacement of dielectric constant after poling into the tetragonal phase can be explained as follows [19].

Let us imagine the dielectric constant before poling of a piezoelectric ceramic as the sum [20]

$$K_r = K_i + K_{or}$$

where K_i is caused by induced polarization and K_{or} by orientational polarization. Thermodynamic investigation [21] provides an explanation of K_i passing through a maximum in the morphotropic region. In addition, proceeding from thermodynamic relationships, the increase in K_i near the morphotropic region may be qualitatively connected with a decrease here of spontaneous polarization, P_s, which is confirmed by a drop in the uniform deformation parameter δ [22].

The decrease in δ there also increases K_{or} due to the growth of mobility of domain boundaries. Some contribution to K_{or} inside the morphotropic region is apparently made by the mobility of boundaries of co-existing phases. All this leads to the formation of a maximum K_r in the vicinity of the morphotropic region.

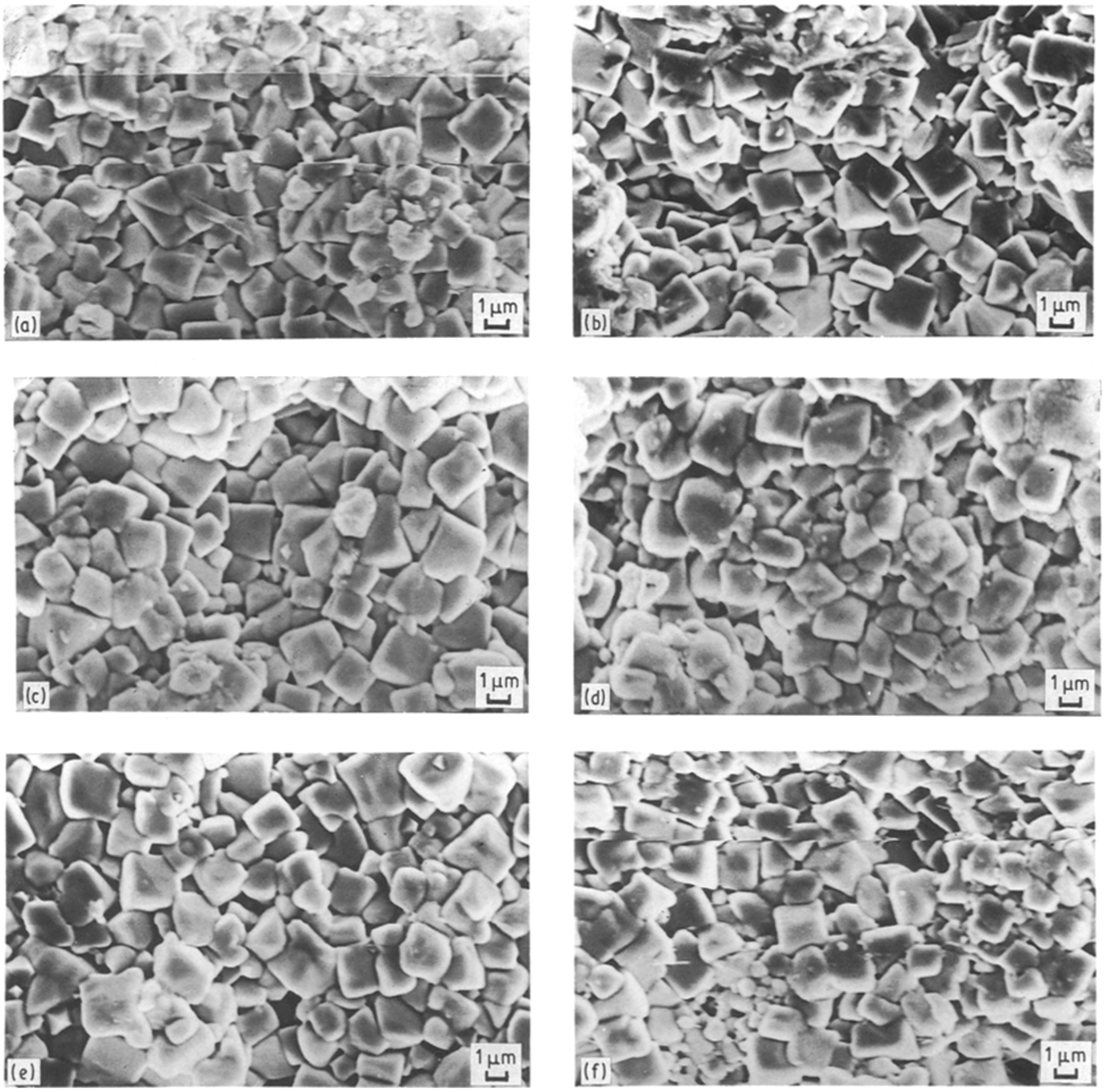

Figure 3 Microstructure of sintered samples of the $Pb_{0.96}Sr_{0.04}[(Ti_xZr_{1-x})_{0.88}(Mn_{1/3}Nb_{2/3})_{0.04}(Zn_{1/3}Nb_{2/3})_{0.08}]O_3$ system with different x values: (a) 0.40, (b) 0.47, (c) 0.49, (d) 0.50, (e) 0.51, (f) 0.53.

As to the maximum of dielectric constant after poling, K^T_{33}, its more pronounced character and displacement into the tetragonal phase may be related to the degree of domain reorientations differing from 180°, η. In the region with higher values of η (pseudocubic), K^T_{33} is decreasing in comparison to K_r as a result of dielectric anisotropy, and in the region with low η (tetragonal) K^T_{33} increases because of relieving the clamping effect. This leads to a rise of dielectric constant in the tetragonal branch and to a reduction in the pseudocubic branch. This effect of the displacement of maximum K^T_{33} outside the morphotropic region, described also by Berlincourt *et al.* [23] and Petrsch and Topf [24], draws attention to the contribution of interphase boundary movement to this maximum, which, however, is taken account of in some investigations.

In this system, the planar coupling factor is related to $PbTiO_3$ concentration as shown in Fig. 5. The variation of coupling factor with composition is the same as that of the dielectric constant, but its maximum value occurs at $x = 0.50$, and then decreases for higher $PbTiO_3$ concentrations. Fig. 5 also shows the variation of the mechanical quality factor Q_m with $PbTiO_3$ concentration. The lowest mechanical quality factor is at the morphotropic phase boundary, where $x = 0.50$. The value of Q_m decreases in the pseudocubic phase with increasing $PbTiO_3$ concentration, but it increases in the tetragonal phase.

The variation of piezoelectric constant d_{33} as a function of Ti composition is shown in Fig. 6. It is found that the piezoelectric constant is high near the MPB region. The maximum value is 181×10^{-12} $C\,N^{-1}$ at $x = 0.50$. In the tetragonal phase, the d_{33} value apparently decreases with increasing Ti concentration, but in the pseudocubic phase a variation of d_{33} is not apparent.

Fig. 6 also shows that the longitudinal velocity has

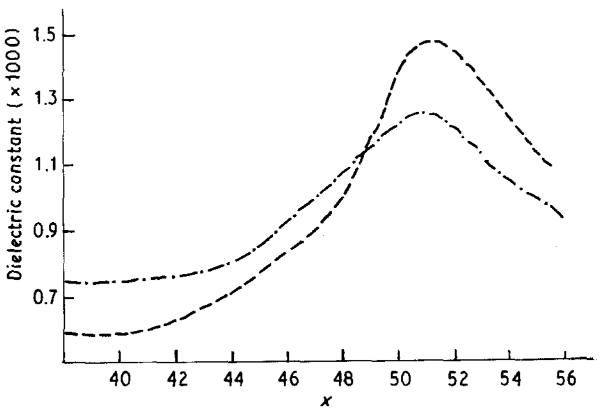

Figure 4 Variation of dielectric constant (—·—) before and (- - -) after poling of the $Pb_{0.96}Sr_{0.04}[(Ti_xZr_{1-x})_{0.88}(Mn_{1/3}Nb_{2/3})_{0.04}(Zn_{1/3}Nb_{2/3})_{0.08}]O_3$ system with different x values.

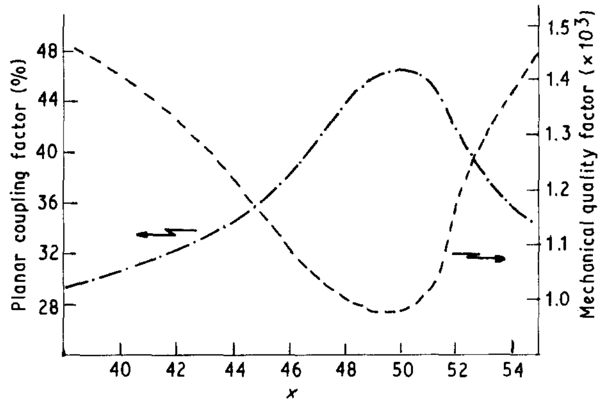

Figure 5 Variation of (—·—) planar coupling factor and (- - -) mechanical quality factor of the $Pb_{0.96}Sr_{0.04}[(Ti_xZr_{1-x})_{0.88}(Mn_{1/3}Nb_{2/3})_{0.04}(Zn_{1/3}Nb_{2/3})_{0.08}]O_3$ system with different x values.

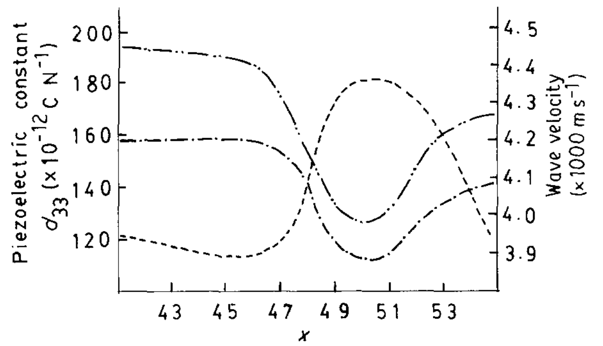

Figure 6 Variation of (- - -) piezoelectric constant d_{33} and longitudinal velocity (—·—) before and (—··—) after poling of the $Pb_{0.96}Sr_{0.04}[(Ti_xZr_{1-x})_{0.88}(Mn_{1/3}Nb_{2/3})_{0.04}(Zn_{1/3}Nb_{2/3})_{0.08}]O_3$ system with different x values.

a minimum value at the phase boundary and the wave velocity is faster after poling. Before polarization the directions of the domain were very random and the domain walls cause scattering of the sound wave. After polarization, most domains are forced along the direction of polarization and the scattering of sound waves is reduced, leading to an increase in the velocity [25]. The reason for the decrease of velocity at the phase boundary is considered to be the existence of a region of different symmetry (DSR). The DSR means that regions of the tetragonal phase are in pseudocubic grains and regions of the pseudocubic phase are in tetragonal grains. Owing to the DSR comprising the tetragonal phase and the pseudocubic phase, the interphase boundary causes extra scattering of the velocity compared to other compositions.

The hysteresis loop is one of the most important characteristics of a ferroelectric and gives information on its dynamic polarization. The P–E curves of the system are shown in Fig. 7. The coercive field (E_c) is nearly constant for the pseudocubic composition, but it increases with increasing $PbTiO_3$ in the tetragonal region. The variation of remanent polarization (P_r) with composition is the same as that of the coupling factor.

In the $Pb_{0.96}Sr_{0.04}[(Ti_xZr_{1-x})_{0.88}(Mn_{1/3}Nb_{2/3})_{0.04}(Zn_{1/3}Nb_{2/3})_{0.08}]O_3$ system, it is found that a high mechanical quality factor ($Q_m = 960$) and lower planar coupling factor ($k_p = 0.47$) occur at the MPB with $x = 0.50$. Takahashi *et al.* [10] deal with the synthesis of $PbZrO_3$–$PbTiO_3$–$Pb(Mn_{1/3}Nb_{2/3})O_3$ ternary ceramic compounds and their piezoelectric properties. They found that the coupling factor depend on the concentration of $Pb(Mn_{1/3}Nb_{2/3})O_3$, and its maximum value was 0.68 for $Pb(Mn_{1/3}Nb_{2/3})O_3$ equal to 8 mol %. Therefore, the following discussion is concerned with the properties of $Pb_{0.96}Sr_{0.04}[(Ti_{0.5}Zr_{0.5})_{1-z}(Mn_{1/3}Nb_{2/3})_z(Zn_{1/3}Nb_{2/3})_{0.08}]O_3$ with $z = 0.04$–0.10.

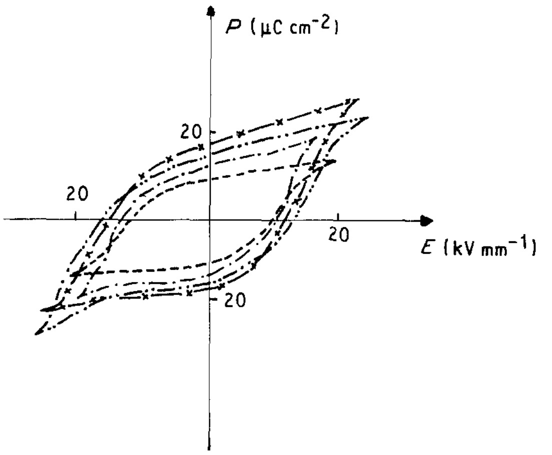

Figure 7 Hysteresis loop of the $Pb_{0.96}Sr_{0.04}[(Ti_xZr_{1-x})_{0.88}(Mn_{1/3}Nb_{2/3})_{0.04}(Zn_{1/3}Nb_{2/3})_{0.08}]O_3$ system with different x values: (- - -) 0.47, (—·—) 0.49, (— × —) 0.50, (—··—) 0.53.

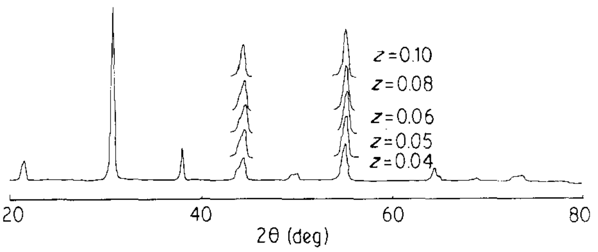

Figure 8 XRD patterns of the $Pb_{0.96}Sr_{0.04}[(Ti_{0.5}Zr_{0.5})_{1-z}(Mn_{1/3}Nb_{2/3})_z(Zn_{1/3}Nb_{2/3})_{0.08}]O_3$ system with different x values.

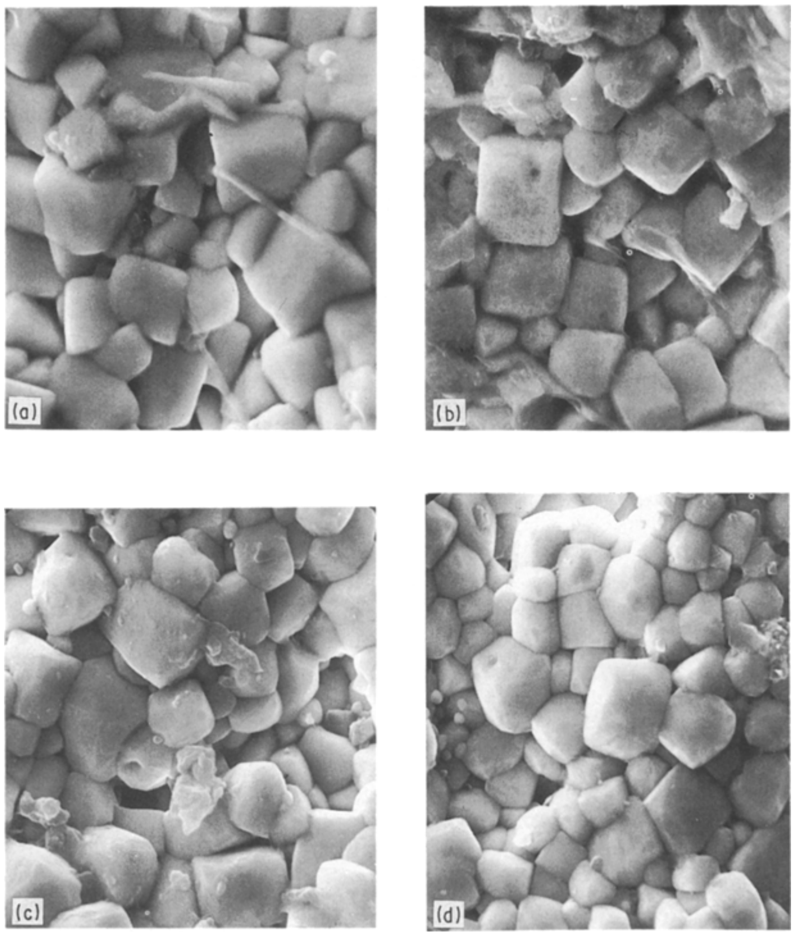

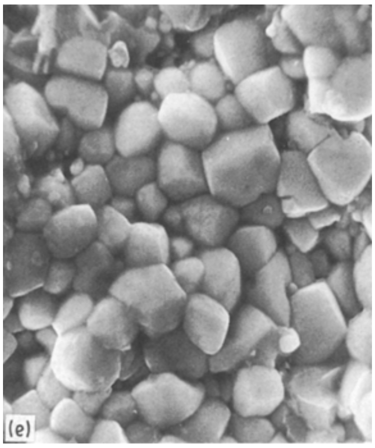

Figure 9 Microstructure of sintered samples of the $Pb_{0.96}Sr_{0.04}$-$[(Ti_{0.5}Zr_{0.5})_{1-z}(Mn_{1/3}Nb_{2/3})_z(Zn_{1/3}Nb_{2/3})_{0.08}]O_3$ system with different z values: (a) 0.04, (b) 0.05, (c) 0.06, (d) 0.08, (e) 0.10.

XRD patterns of the system with different amounts of $Mn_{1/3}Nb_{2/3}$ are shown in Fig. 8. In these patterns, the perovskite phase is all of pseudocubic symmetry and no pyrochlore phase can be found.

Typical microstructures are given in Fig. 9. Because the ions of Nb and Mn are inhibitors of grain growth [25, 26], so the grain size gradually becomes smaller with increase of $Mn_{1/3}Nb_{2/3}$ concentration.

The relation of planar coupling factor with $Mn_{1/3}Nb_{2/3}$ concentration is shown in Fig. 10. From this figure, it is found that the planar coupling factor reaches a maximum value near 5 mol %.

Fig. 10 also shows the variation of mechanical quality factor (Q_m) and dielectric loss ($\tan\delta$) with $Mn_{1/3}Nb_{2/3}$ concentration. The mechanical quality factor as well as dielectric loss increase with an increase of $Mn_{1/3}Nb_{2/3}$.

The relation of dielectric constant and composition is also shown in Fig. 10. The results are in contradiction to those for Q_m and dielectric loss.

The piezoelectric constant d_{33} reaches its highest value of 251×10^{-12} C N^{-1} at 6 mol % $Mn_{1/3}Nb_{2/3}$, as also shown in Fig. 10.

Through the above-mentioned results, it may be supposed that the improving effects on piezoelectric properties taking place through variation of $Mn_{1/3}Nb_{2/3}$ concentration are due to the different

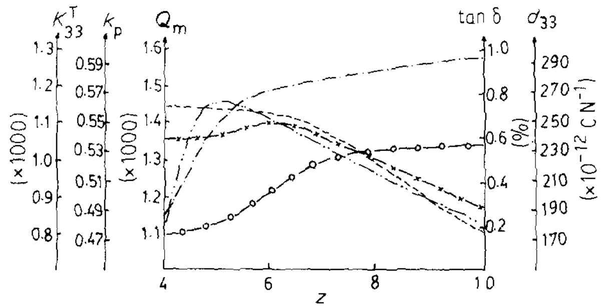

Figure 10 Variation of (– – –) dielectric constant K_{33}^T, (—··—) planar coupling factor k_p, (—·—) mechanical quality factor Q_m, (—o—) dielectric loss $\tan\delta$ and (– × –) piezoelectric constant d_{33} of the $Pb_{0.96}Sr_{0.04}[(Ti_{0.5}Zr_{0.5})_{1-z}(Mn_{1/3}Nb_{2/3})_z(Zn_{1/3}Nb_{2/3})_{0.08}]O_3$ system with different z values.

amount of space charge generated in the compound, resulting from the coexistence of manganese ions and niobium ions [7].

4. Conclusions

There are two phases existing in the (Pb, Sr)[(Zr, Ti) $(Mn_{1/3}Nb_{2/3})$ $(Zn_{1/3}Nb_{2/3})$] O_3 piezoelectric ceramic: one is tetragonal and the other is pseudocubic. With a constant amount of 4 mol % $Pb(Mn_{1/3}Nb_{2/3})O_3$ and 8 mol % $Pb(Zn_{1/3}Nb_{2/3})O_3$, the MPB exists when the amount of $PbTiO_3$ is nearly equal to 44 mol %. The structure is perovskite with pseudocubic symmetry for $PbTiO_3$ less than 44 mol %, but it is tetragonal symmetry for higher $PbTiO_3$ concentrations. The sintered density is greater than 94% of theoretical density.

The planar coupling factor ($k_p = 0.47$) and piezoelectric constant ($d_{33} = 181 \times 10^{-12}\,CN^{-1}$) are higher at compositions near the MPB but the mechanical quality factor, frequency constant and longitudinal velocity are lowest.

In piezoelectric ceramics, depending on the crystalline phase, the dielectric constant may increase or decrease through poling treatment. In this system the dielectric constant is increased for the tetragonal compositions but decreased for the pseudocubic compositions after poling. As far as the dielectric constant of poled ceramic is concerned, its maximum in the multicomponent system is displaced into the tetragonal phase and does not coincide with the maximum of electromechanical quality factor. Before and after poling, compositions close to the MPB are characterized by the smallest velocity of the longitudinal sound wave. Further, the longitudinal wave velocity of poled samples is higher than that of unpoled ones.

The hysteresis loop gives information on the dynamic polarizability. The coercive field (E_c) is nearly constant for pseudocubic compositions but it will increase with increasing $PbTiO_3$ in the tetragonal region. The variation of remanent polarization with composition is the same as that of the coupling factor. Thus, compositions with the tetragonal phase are "ferroelectrically harder" and those with the pseudocubic phase are "ferroelectrically softer" than compositions close to the MPB.

From XRD, we conclude that the compositions $Pb_{0.96}Sr_{0.04}$ $[(Zr_{0.5}Ti_{0.5})_{1-z}$ $(Mn_{1/3}Nb_{2/3})_z$ $(Zn_{1/3}Nb_{2/3})_{0.08}]O_3$ with $z = 0.04$–0.10 are in the pseudocubic phase region. The grain size becomes smaller with increase of $Mn_{1/3}Nb_{2/3}$ concentration. The planar coupling factor ($k_p = 0.57$) and piezoelectric constant ($d_{33} = 251 \times 10^{-12}\,CN^{-1)}$ reach a maximum at 5 and 6 mol % $Mn_{1/3}Nb_{2/3}$, respectively. The mechanical quality factor and loss tangent are increased, but the dielectric constant decreases, with increasing $Mn_{1/3}Nb_{2/3}$.

References

1. T. IKEDA, *J. Phys. Soc. Jpn* **14** (1959) 168.
2. F. KULCSAR, *J. Amer. Ceram. Soc.* **42** (1959) 49.
3. B. JAFFE, R. S. ROTH and S. MARZULLO, *J. Res. Natl. Bur. Std.* **55** (1955) 239.
4. F. KULCSAR, *J. Amer. Ceram. Soc.* **42** (1959) 343.
5. M. MARUTAKE, Japanese Patent 16673 (1961).
6. F. KULCSAR, US Patent 3006857 (1961).
7. H. OUCHI, K. NAGANA and S. HAYAKAWA, *J. Amer. Ceram. Soc.* **48** (1965) 630.
8. T. KUDO, Y. YAZAKI, F. NAITO and S. SUGAYA, *ibid.* **53** (1970) 326.
9. M. TAKAHASHI and TAKAHASHI, US Patent 3699045 (1972).
10. M. TAKAHASHI, N. TSUBOUCHI, M. YONEZAWA, T. OHNO and T. AKASHI, *NEC Res. Devel.* **35** (1974) 57.
11. J. P. GUHA and D. J. HONG, *J. Amer. Ceram. Soc.* **71** (1988) C-152.
12. P. Gr. LUCUTA and D. BARB, *ibid.* **68** (1985) 533.
13. S. S. CHANG and J. A. PARK, *ibid.* **60** (1979) 684.
14. C. B. SAWYER and C. H. TOWER, *Phys. Rev.* **35** (1930) 269.
15. "IRE Standards on Piezoelectric Crystal: Measurement of Piezoelectric Ceramic, 1961", *Proc. IRE* **49** (1961) 1161.
16. V. A. ISUPOV and Yu. E. STOLYPIN, *Sov. Phys. – Solid State* **11** (1969) 2067.
17. V. A. ISUPOV, *ibid.* **10** (1968) 989.
18. Z. Q. ZHUANG, M. J. HAUN, S. J. JANG and L. E. CROSS, in Proceedings of 1986 IEEE 6th International Symposium on Application of Ferroelectrics (1986) p. 394.
19. E. G. FESENKO, A. YA DANTSIGER, L. A. RESNITCHENKO and M. F. KUPRIYANOV, *Ferroelectrics* **41** (1982) 137.
20. V. A. BOKOV, *J. Technicheskoy Fiziki* **27** (1957) 1784.
21. K. CARL and K.H. HARDTL, *Phys. Status Solidi (a)* **8** (1971) 87.
22. M. Ya. SHIROBOKOV and L. P. KHOLODENKO, *J. Technicheskoy Fiziki* **27** (1951) 1239.
23. D. A. BERLINCOURT, C. CMOLIC and H. JAFFE, *Proc. IRE* **48** (1960) 220.
24. K. PETRSCH and K. J. TOPF, *Ber. Dt. Kerem. Ges.* **47** (1970) 681.
25. P. S. NICHOLSON and N. D. PATEL, *Amer. Ceram. Soc. Bull.* **65** (1986) 783.
26. H. T. MARTIRENA and J. C. BURFOOT, *J. Phys. C: Solid State Phys.* **7** (1974) 3182.

Received 23 April
and accepted 19 November 1990